

## Research Article

# Accurate Clamping Method of Multipoint Flexible Fixture for Large Complex Surface

Ruolong Qi <sup>1,2</sup>, Xinyuan Mao <sup>1</sup>, Ke Zhang <sup>1</sup> and Renbo Xia <sup>2</sup>

<sup>1</sup>School of Mechanical Engineering, Shenyang Jianzhu University, Shenyang, Liaoning, China

<sup>2</sup>The State Key Laboratory of Robotics, Shenyang Institute of Automation, Chinese Academy of Sciences, Shenyang, Liaoning, China

Correspondence should be addressed to Ruolong Qi; qiruolong@126.com

Received 19 February 2021; Accepted 10 July 2021; Published 19 July 2021

Academic Editor: Z. Du

Copyright © 2021 Ruolong Qi et al. This is an open access article distributed under the Creative Commons Attribution License, which permits unrestricted use, distribution, and reproduction in any medium, provided the original work is properly cited.

In the field of aviation and astronautics, large complex surface parts such as aircraft cabin cover are complex, varying in model, and produced in small batch. In order to reduce fixture cost and improve production efficiency, a variable multipoint and multi-DOF supporting fixture is designed. The coordinate system of the complex structure fixture is defined, and the kinematics of the multibody structures driven by air cylinders are modeled according to the topological principle. With the help of this data structure, fast and optimal search for clamping state can be realized. With the dichotomy method, the driving amount of the electric cylinder of the suction cups and the two rotation angles of two rotation axes at the end of the linkages are solved accurately. Based on the digital twin simulation method, the precise clamping motion of flexible fixture is calculated for an aircraft cockpit cover with a software developed by the authors in C++ language on the Visual studio platform. The distance between the clamping point and the surface was verified with a laser tracker. Finally, the practical experiment of a real cockpit cover clamping proves the practicability and effectiveness of the proposed method.

## 1. Introduction

In the field of modern high-end manufacturing, more and more large thin-walled complex surface parts are used in aerospace vehicles, such as aircraft skin and cockpit cover. The machining process of every large complex part requires several suitable supporting fixtures, which were usually manufactured by the machine tools according to the numerical models. However, this kind of rigid complex surface fixture has low process flexibility, low utilization rate, and high manufacturing cost, which has become a burden in the field of aerospace manufacturing.

At present, there are hundreds of types of cockpit covers produced in China, and each type has different specific models. In the production of various kinds of cockpit cover, the multipoint supporting flexible fixture is an important means to solve the problem of quick replacement of clamping. However, for the cockpit covers with different sizes, shapes, and curvature changes, how to realize fast and

accurate digital clamping and the displacement calculation of multipoint and multidegree of freedom system are the key problems to be solved urgently.

The traditional fixture adopts the six-point positioning principle, positioning parts with its own high-precision positioning components [1]. However, with the increase of complex surface parts in aerospace field, more and more flexible fixtures for complex surface parts appear. Most flexible fixtures were designed as rod-type structure, which used a number of support rods arranged in rows and columns to form different shapes with varying heights [2]. The advantage of this classic flexible fixture lies in its clear structure and simple control model. Its supporting motion only has vertical upward degrees of freedom. However, its limitation lies in that it can only support the open surface with small curvature change and low crimp degree [3]. In order to improve the control precision of the flexible fixture, the current scholars have made a lot of efforts, and there are mainly two methods to improve the control precision. The

first method is the detection method based on contact control. Zhan and Zhou [4] developed an adaptive sliding mode method to detect the contact between the support rod and the workpiece. Zhou et al. [5] proposed a gripping force control method based on force perception interaction of virtual model, but it was extremely difficult to match virtual model with real workpiece. The clamping accuracy is precisely controlled by the precise control of the clamping force. This precision control method has high contact precision, but for thin-walled parts that are easy to deform, this clamping control method cannot correct the deformation [6].

The second method is based on a measurement correction method. Due to the inaccuracy of the clamping position, Do et al. [7] proposed the clamping pose measurement method based on vision measurement, and the clamping correction amount can be given out. Hao et al. [8] applied the contact measurement method to obtain the actual clamping state of the workpiece and finally optimized the fixture by minimizing the error distribution. The positioning matching method of machining track for the complex surface on fixture proposed by Xu et al. [9, 10] is also based on measurement.

Besides the fixture with support point matrix, there is also a fixture with expandable connecting rod structure to clamp the thin wall surface. This new flexible fixture has been designed based on the principle of multiple dynamic vibration [11]. It is a special fixture used only for clamping the casing of the aircraft engine [12]. In order to improve the rigidity of the clamping system and reduce the vibration of the system, a certain optimization method is usually used to optimize the clamping position of the fixture [13, 14]. In addition to the mechanical fixture, there is now a magnetic fluid fixture [15]. This clamping method is based on the magnetorheological principle, which can be used to clamp any shape in theory, but the problem of its practical application remains to be further studied.

In this paper, a variable multipoint, multidegree of freedom flexible fixture is designed. The coordinate system of the fixture is introduced, and the mathematic description model of the fixture movement process is established based on the topological theory. The optimal clamping position of complex faceless parts was determined by bounding box matching method and multibranch tree depth-first traversal, and the clamping position was accurately calculated by binary iteration. The fixture designed in this paper can hold dozens of aircraft cabin cover parts with strong compatibility. Its innovation lies in the accurate calculation of the clamping position through the combination of virtual fixture and real fixture, which not only has high clamping accuracy, but also has a suppressing effect on the deformation of thin-walled complex surface. In this paper, a method combining topological theory with complex surface positioning on flexible fixture is proposed, which greatly improves the automation ability of flexible fixture and the accuracy of clamping.

The remainder of this work is organized as follows. Section 2 introduces the structure of the new flexible fixture. In Section 3, an accurate clamping method is described. In

the fourth part, the authors give the virtual simulation software and the realization of the precise clamping method based on the software. Then, the cockpit cover is clamped with practical tooling. Finally, Section 5 concludes the paper and proposes future studies.

## 2. Fixture Structure

**2.1. Mechanical Structure.** The main structure of the fixture is composed of two parts: the fixture body and the fixture base. As shown in Figure 1(a), the fixture body has three clamping boards, in which the fixed board is fixed on the fixture base and cannot be moved. However, the front board and the back board can move forward and backward with a certain distance driven by air cylinders on the fixture base.

Each fixture board has five orthogonal translational substructures as shown in Figure 1(b). The middle suction cup can only be driven up and down by the electric cylinder, and the other four suction cups can also be up and down, but they also can move left and right driven by the air cylinders with a certain distance. So, for the three clamping boards, there are a total of 15 suction cups. The detailed orthogonal structure of each suction cup is shown in Figure 2. Three translational mechanisms and two rotary mechanisms constitute a small five-axis system. A suction cup can move in three-dimensional space, when the  $\vec{x}$  and  $\vec{y}$  axes are driven by air cylinders, and  $\vec{z}$  axis is driven by electric cylinders. The two rotation axes of  $\vec{x}$  and  $\vec{z}$  intersect at one point to form a mechanism that approximates a spherical linkage. This mechanism that can change the direction of the suction cup freely and the orthogonal mechanism together form flexible clamp for the aircraft cockpit cover with different sizes and shapes.

**2.2. Coordinate Definition.** It can be seen from the structure of the flexible fixture that it is a typical multibody linkage system. In order to establish the mathematical motion modeling of the flexible fixture, it is necessary to establish the topological model of the mechanism from the perspective of motion and simulation to describe the kinematic correlation between the structures.

As shown in Figure 3, the whole fixture is a tree structure, in which the base coordinate  $T_{\text{base}}$  is the global coordinate for the entire system. The front board coordinate  $T_{f0}$ , the middle board coordinate  $T_{m0}$  and the back coordinate  $T_{b0}$  are the local coordinates of the fixture boards, whose transformation matrixes from the base coordinate are  $T_f^{\text{base}}$ ,  $T_m^{\text{base}}$  and  $T_b^{\text{base}}$  respectively. They are the second layer of the structure.

$$\begin{cases} T_{f0} = T_{\text{base}} \cdot T_f^{\text{base}}, \\ T_{m0} = T_{\text{base}} \cdot T_m^{\text{base}}, \\ T_{b0} = T_{\text{base}} \cdot T_b^{\text{base}}. \end{cases} \quad (1)$$

The initial states of the suction cup coordinates  $T_{fi}$ ,  $T_{mi}$  and  $T_{bi}$  ( $i = 1, \dots, 5$ ) are the third layer of the structure tree. From the board coordinates to the coordinates of the suction cups, the transformation relations can be written as

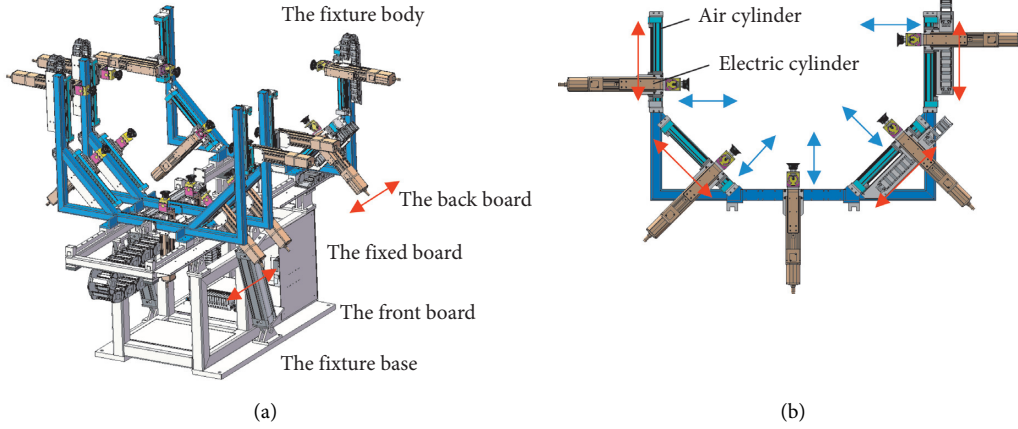


FIGURE 1: Concrete structure of the fixture. (a) Main structure of the fixture. (b) Substructure of the fixture board.

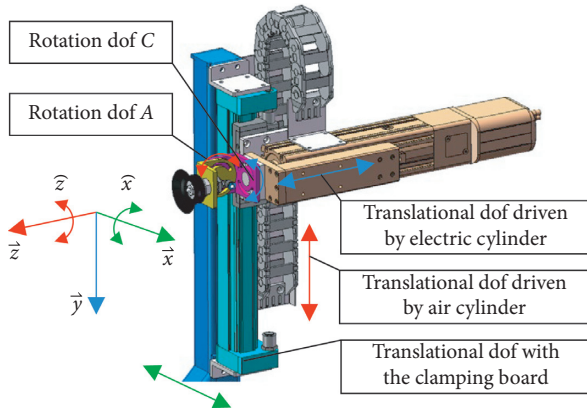


FIGURE 2: Detailed structure of the fixture.

$$\begin{cases} T_{fi} = T_{f0} \cdot T_{fi}^f \\ T_{mi} = T_{m0} \cdot T_{mi}^m, & (i = 1, \dots, 5). \\ T_{bi} = T_{b0} \cdot T_{bi}^b, \end{cases} \quad (2)$$

Since the middle clamping board is fixed, so the transformation matrix  $T_m^{\text{base}}$  is a constant value. In this project, the base coordinate coincides with the coordinate of the middle clamping board. So  $T_m^{\text{base}}$  is an augmented identity matrix.

$$T_m^{\text{base}} = I_{4 \times 4}. \quad (3)$$

As shown in Figure 3, for the front and back clamping board, their movements are all along the  $x$  direction of the base coordinate.

$$T_f^{\text{base}} = T_b^{\text{base}} = \begin{bmatrix} I_{3 \times 3} & \vec{m} \\ 0 & 1 \end{bmatrix}, \quad (4)$$

in which  $\vec{m} = [l_x \ 0 \ 0]$ ,  $l_x$  is the extension length of the air cylinder that drives the clamping board. When the two clamping boards move forward,  $l_x$  is positive, and when they move backward, it is negative.

The translational movement matrix of each suction cup  $T_{f,i}$ ,  $T_{m,i}$ ,  $T_{b,i}$  includes two variables.

$$T_{f,i}, T_{m,i}, T_{b,i} = \begin{bmatrix} & 0 \\ I_{3 \times 3} & l_y \\ & l_z \\ 0 & 0 & 0 & 1 \end{bmatrix}, \quad (5)$$

in which  $l_y$  is the extension length of the air cylinders that drive the suction cups. The  $l_y$  values of the motion of a pair of suction cups distributed symmetrically on the clamping boards are negative for each other.  $l_z$  is the extended length of the electric cylinder to drive the sucker to hold the cockpit cover.

### 3. Multipoint Clamping Method

Hundreds of types of cockpit covers' model were established in different coordinates by different designers as shown in Figure 4(a). When the workpiece model and the fixture model were imported into the same coordinate frame, their relative postures are unknown. Figure 4(b) illustrates a case in which the relative relationship is unknown after the models are imported. It is necessary to find an automatic positioning matching clamping method so as to calculate the precise movement of each suction cup on the complex surface.

**3.1. Initial Positioning.** It is assumed that the vertex set on the bounding box of the cockpit cover is  $\{P\} = P_i (i = 1, \dots, 8)$ . And the points set on the max bounding box of the suction cup positions is  $\{Q\} = Q_i (i = 1, \dots, 8)$ . The initial positioning of the cockpit cover is to calculate the transforming matrix  $M_{tr}$  between the cockpit cover and the suction cups. An augmented transforming matrix  $M_{tr}$  can be written as

$$T_{tr} = \begin{bmatrix} R_{3 \times 3} & T_{3 \times 1} \\ 0 & 1 \end{bmatrix}. \quad (6)$$

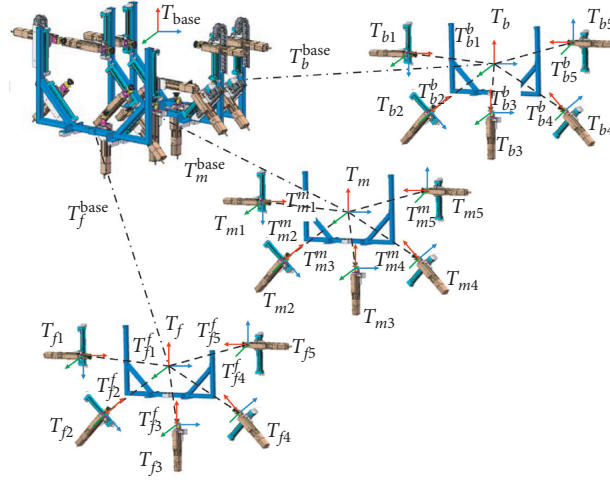


FIGURE 3: Structure topological model and coordinate relations.

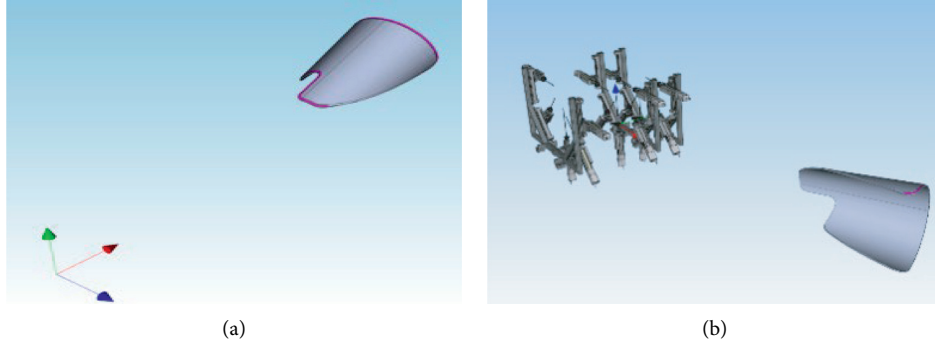


FIGURE 4: The uncertain position and pose relationship between the workpiece and the fixture in the unified coordinate system. (a) Workspace coordinate. (b) Initial import state without positioning.

The mathematical expression to minimize the two set of points can be written as

$$\prod = \frac{1}{2} \sum_i^n \|q_i - Rp_i - T\|^2. \quad (7)$$

This is an optimization problem, which can be solved by several typical algorithms [16]. With the result of  $M_{tr}$ , the two-coordinate frame can coincide to each other. The matching effect is shown in Figure 5.

**3.2. Topology Model.** After initial positioning, it is necessary to carry out an optimized positioning process. Because the clamping position of the clamping board and the suction cup can be spatially driven by air cylinder to form many clamping states, the clamping states can be described by a topology model.

The middle clamping board is fixed, and the other two boards both have two working locations. The working locations are numbered in binary as Figure 6 shows. The position close to the center clamping board has a smaller clamping range and is marked as 0, while the station far away from the center clamping board is marked as 1. The front

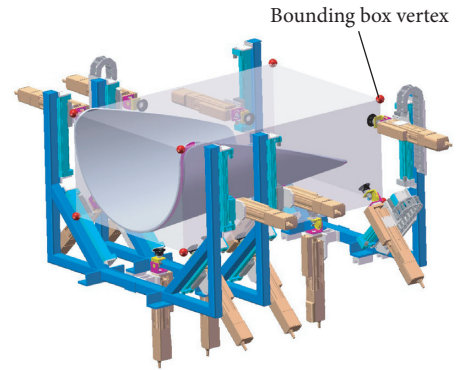


FIGURE 5: Bounding box vertex matching.

clamping board corresponds to the high binary bit, and the rear gripper corresponds to the low binary bit.

It is assumed that the distance that the air cylinder drives the clamping board is  $l_x$ . Then, the movement transformation matrix of the front clamping board corresponding to the bit state 1  $Tr_f^1$  and the movement transformation matrix of the back clamping board corresponding to the bit state 0  $Tr_b^0$  can be written as

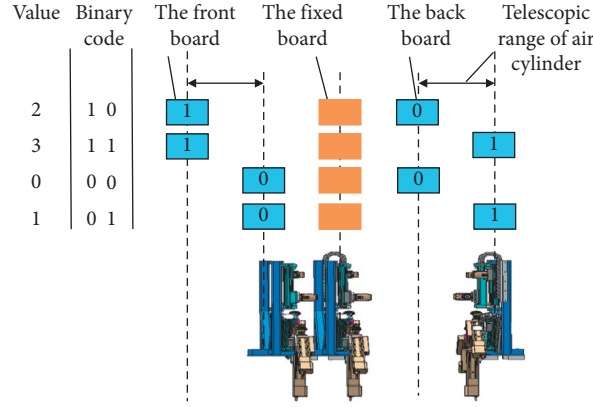


FIGURE 6: Binary encoding of clamping board positions.

$$\text{Tr}_f^1 = \text{Tr}_b^0 = \begin{bmatrix} l_x & 0 \\ l_{3 \times 3} & 0 \\ 0 & 0 & 0 & 1 \end{bmatrix}. \quad (8)$$

Then, the opposite movement transformation matrix  $\text{Tr}_f^0$  and  $\text{Tr}_b^1$  is

$$\text{Tr}_f^0 = \text{Tr}_b^1 = \begin{bmatrix} -l_x & 0 \\ l_{3 \times 3} & 0 \\ 0 & 0 & 0 & 1 \end{bmatrix}. \quad (9)$$

The current position and posture  $T_f$  and  $T_b$  of the front or back clamping board can be calculated as

$$\begin{cases} T_f = T_{f0} \cdot T_f^f = T_{\text{base}} \cdot T_f^{\text{base}} \cdot \text{Tr}_f^j \\ T_m = T_{m0} = T_{\text{base}} \cdot T_m^{\text{base}} \\ T_b = T_{b0} \cdot \text{Tr}_b^j = T_{\text{base}} \cdot T_b^{\text{base}} \cdot \text{Tr}_b^j \end{cases}, \quad (j = 0 \text{ or } 1). \quad (10)$$

For a clamping board, there are five suction cups, in which the clamping direction of the middle one is fixed. Opposing pairs of the left four suction cups form two groups. The top pair is defined as the binary high bit, and the bottom pair as the binary low bit. At each binary bit, the high position of the suction cup is defined as 1, and the lower position as 0. Both the binary code of the clamping board and the binary code of the suction cup in each board have a common feature. As Figure 7 shows, they form four binary codes, and these binary codes correspond to decimal 0~4. The code is set in such a way that the larger the corresponding decimal value, the larger the clamping range.

According to the distribution structure of clamping boards and suction cups, a two-layer topological tree as shown in Figure 8 is formed. The first layer is the clamping board structure with four position choices. The second layer is the suction cup structure with four position choices for every clamping board. The optimal clamping state can be estimated and searched by depth-first traversal in the topological tree.

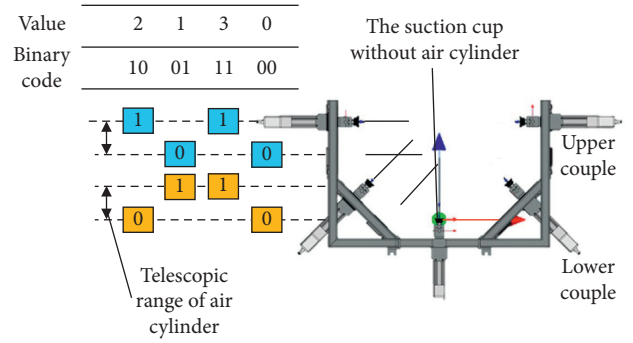


FIGURE 7: Binary encoding of cockpit covers in a clamping board.

It is assumed that the distance that the air cylinder drives the orthogonal mechanism is  $l_y$ . Then, the movement transformation matrix of the suction cups in the front, middle, and back clamping board  $\text{Tr}_{f,i}^1$ ,  $\text{Tr}_{m,i}^1$  and  $\text{Tr}_{b,i}^1$  corresponding to the bit state 1 can be written as

$$\text{Tr}_{f,i}^1 = \text{Tr}_{m,i}^1 = \text{Tr}_{b,i}^1 = \begin{bmatrix} 0 & l_y \\ l_{3 \times 3} & 0 \\ 0 & 0 & 0 & 1 \end{bmatrix}. \quad (11)$$

Then, the opposite movement transformation matrixes  $\text{Tr}_{f,i}^0$ ,  $\text{Tr}_{m,i}^0$  and  $\text{Tr}_{b,i}^0$  corresponding to the bit state 0 can be written as

$$\text{Tr}_{f,i}^0 = \text{Tr}_{m,i}^0 = \text{Tr}_{b,i}^0 = \begin{bmatrix} 0 & -l_y \\ l_{3 \times 3} & 0 \\ 0 & 0 & 0 & 1 \end{bmatrix}. \quad (12)$$

For each combination in the topological tree, test the number of points, at which there is a vector that the suction cup pointers intersect with the cockpit cover surface. It is assumed that the number of intersections is  $n$ . Calculate the volume of the minimum bounding box of the intersections  $V_b$ .

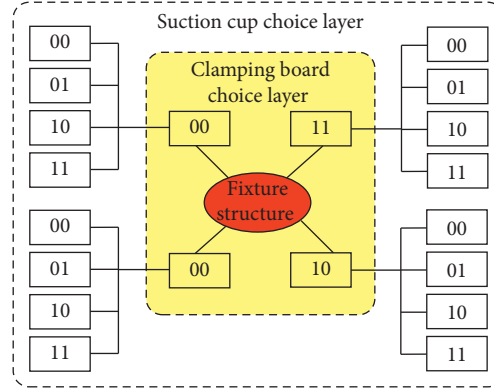


FIGURE 8: The uncertain position and pose relationship between.

$$V_{ave} = \frac{V_b}{n}. \quad (13)$$

$V_{ave}$  approximates the effective volume supported by each suction cup. Choose the topological node with the maximum  $V_{ave}$  as the optimal clamping status [17].

**3.3. Offset Intersection.** After the clamping position is obtained, the motion of the linkage and the rotational momentum of the two rotation angles of the suction cups need to be solved accurately.

Since the aircraft cockpit canopy is a complex surface in space, the clamping direction of the suction cup should be consistent with the normal vector of the clamping point. The two rotation axes of a suction cup intersect at a point. The aim is to calculate the extended distance of the intersection point and the two rotation angles of the axes. As shown in Figure 9, the initial position is  $p_0$  and the distance between the end surface of the suction cup and the intersection point of the rotating shafts is  $d$ . The clamping process is to find a point  $p_a$  that has a  $d$  distance from the surface along the vector of the electric driver direction.

The dichotomy solution process is shown in Figure 10. The distance from the starting point  $p_0$  to the intersection point  $p_e$  is bisected, and the distance from the midpoint  $p_m$  to the surface is calculated. If the projected distance  $d_m$  is greater than the set distance  $d$ , set the middle point  $p_m$  as the end point and vice versa. Thus, the calculation process is iterated until the error between the distance from some intermediate point to the surface and the set distance  $d$  is less than a tiny value  $\varepsilon$  which is almost always set to 0.01 mm.

**3.4. Digital Twin Simulation.** Under the Visual Studio platform, the digital twin system is written in C++ language, as shown in Figure 11. All the algorithms proposed in this paper were realized in this software.

The clamping calculation details are shown in Figure 12. The figure clearly shows the intersection of the clamping linkage vector and the cockpit cover surface, as well as the space line segment with a projected distance  $d$ .

In order to compare the effectiveness of the theoretical position calculated by the algorithm in this paper in actual

clamping, an API laser tracker is used to measure the actual clamping position. A target ball seat of the laser tracker is designed in the center of each vacuum sucker of the flexible fixture. Control the flexible fixture to move to the clamping position, and measure the clamping position with the laser tracker as shown in Figure 13. The measured points are measured in the measurement coordinate system of the laser tracker, and the theoretical clamping positions are calculated by the algorithm in the coordinate system of the fixture. Since they are in different coordinate systems, IPC matching algorithm can be used for error matching and evaluation. By matching and comparing the measurement points with the mathematical model of the complex surface, the maximum error between them is measured, so as to verify the clamping accuracy [18]. The mathematical models of the surface and the measurement points are shown in Figure 14. The measured clamping positions and their corresponding position errors are shown in Figure 15. The clamping errors measured by the laser tracker are shown in Table 1.

From the experiment result, it can be seen that the clamping errors are within the range of 0.01~0.06 mm. Since the vacuum suction plate has a certain elasticity, this small error can be compensated by the elasticity of the vacuum chuck. From the point of view of mathematical calculation, the calculation error should be in micron level [19]. The actual measurement error includes the manufacturing and assembling error of the flexible fixture.

**3.5. Complex Surface Clamping Experiment.** The flexible workpiece is used for clamping various types of cockpit covers. The cockpit cover of a new type of coach plane is used as the experimental object. The cockpit cover is placed on the flexible clamping tool, and the clamping calculation is carried out by the algorithm proposed in this paper.

The states before and after clamping are shown in Figures 15(a) and 15(b). The clamped cockpit cover is extremely stable on the flexible workpiece. According to the position of the workpiece determined by the fixture, the machining process of the cockpit cover is good, which fully proves the correctness and practicability of the method presented in this paper.



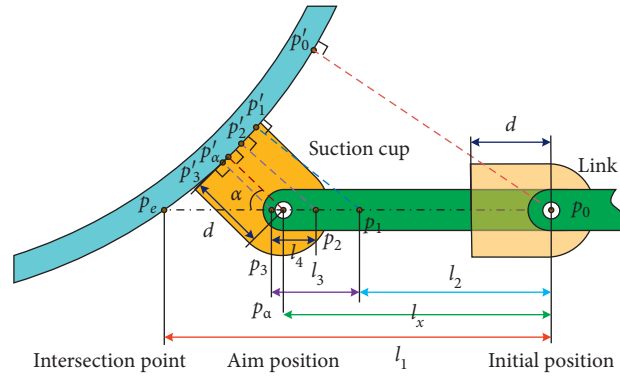


FIGURE 9: The dichotomy method used to solve the clamping position.

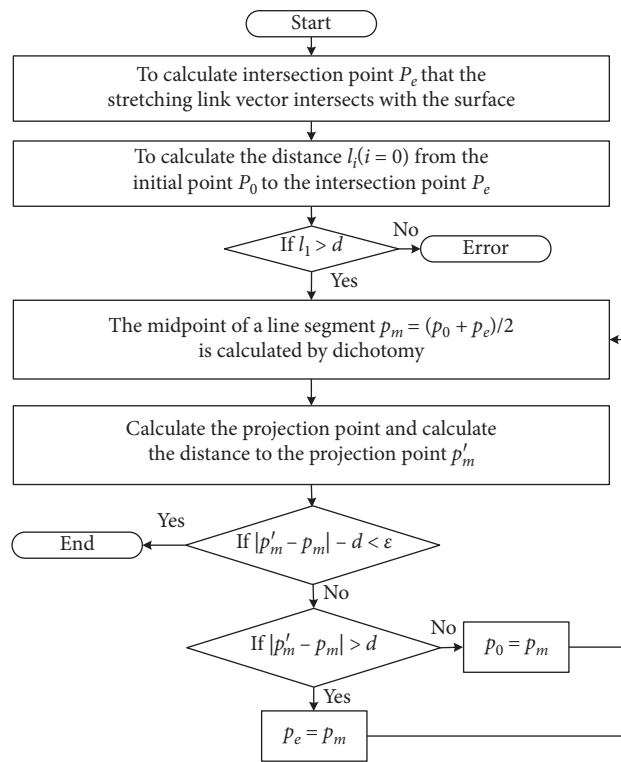


FIGURE 10: The dichotomy solution process.

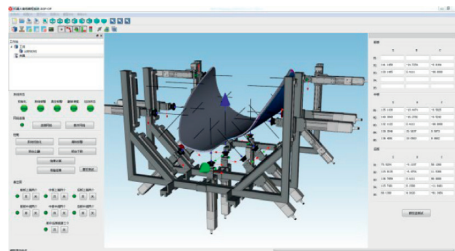


FIGURE 11: Digital twin software system.

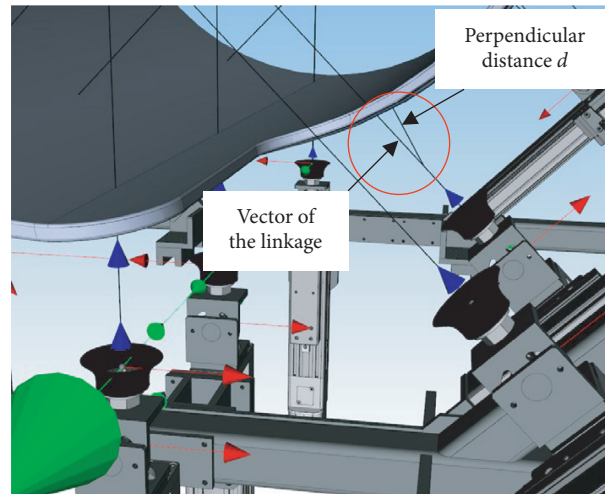


FIGURE 12: Clamping calculation details.



FIGURE 13: Clamping accuracy measurement.

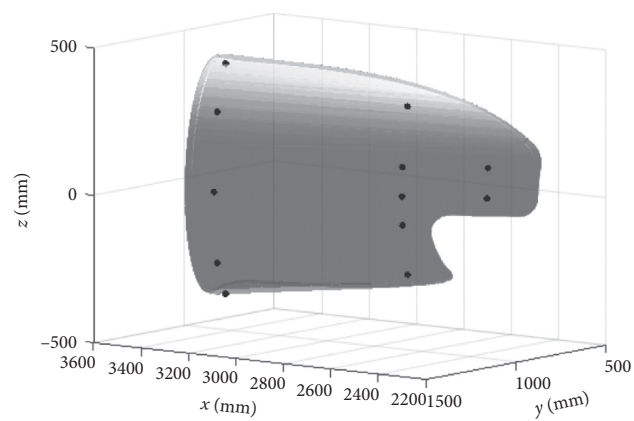


FIGURE 14: Clamping point matching results.



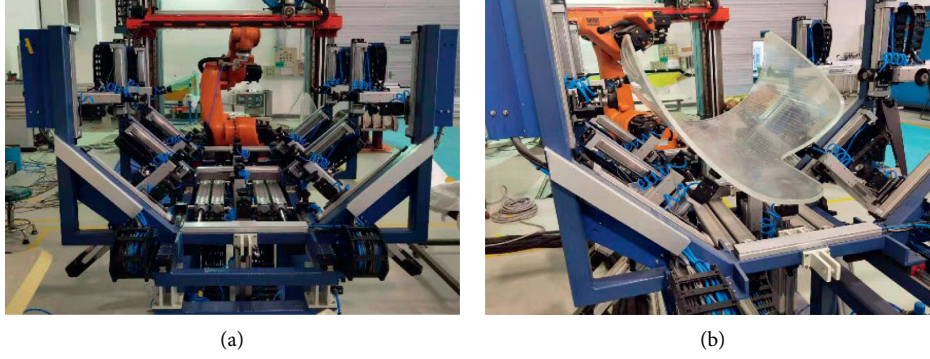


FIGURE 15: Clamping experiment. (a) System state before clamping. (b) Clamping experiment of the cockpit cover.

TABLE 1: The measured value of the clamping error.

Item	Positions (mm)	Error (mm)
P1	[2831.1395, 772.9847, 284.2771]	0.0238
P2	[2766.7097, 884.5273, 98.2677]	0.0534
P3	[2759.7418, 896.5880, 0.0000]	0.0254
P4	[2767.0635, 883.9120, -100.6896]	0.0359
P5	[2832.3467, 770.8969, -286.0653]	0.0494
P6	[2510.5530, 748.5794, 101.2820]	0.0266
P7	[2502.6377, 762.2407, 0.0000]	0.0223
P8	[3481.0746, 925.5515, 390.6329]	0.0055
P9	[3373.7854, 1112.1925, 256.9174]	0.0087
P10	[3327.2485, 1193.1330, 0.0000]	0.0222
P11	[3373.0746, 1113.4285, -255.2019]	0.0481
P12	[3479.8492, 927.6684, -390.0309]	0.0547

## 4. Conclusions

This paper introduces a precise clamping method of multipoint flexible fixture in detail. Aiming at the unknown difference between the coordinate system of flexible fixture and the coordinate system of the workpiece model, a matching method based on the feature points of bounding boxes was proposed. Based on the topological theory, a tree data structure was established for the complex movement of flexible fixture, and the feasible clamping methods were searched based on depth-first traversal. Based on the empirical function of optimal clamping, the available clamping modes were screened, and the optimal clamping modes were obtained. On this basis, the equidistant clamping position perpendicular to the complex surface is calculated by the dichotomy iteration strategy. The simulation and experiment based on the cockpit covers demonstrate the correctness and practicability of the proposed method.

Different from most flexible fixture, the fixture in this paper is a variable complex series-parallel mechanism, and the drive mode is a mixture of pneumatic step type and electric feed type. The innovation of this paper lies in the establishment of multibranch tree model based on topological theory. The advantage of this topology model is that it clearly shows the connection relationship between the various moving parts of the fixture and includes a variety of control methods. The application of topology can well describe the clamping state of the complex flexible fixture.

This paper also proves that topology is particularly suitable for the description of the mechanisms of variable structures in engineering. The method proposed in this paper is different from the traditional fixture clamping strategy. The traditional fixture determines how to position firstly, which is a method that positions before matching. But the method proposed in this paper is to determine the best positioning strategies and then constrains the shape of the complex surface workpiece with the flexible fixture, which can be defined as a method that matches before positioning.

The next research will explore the relationship between the clamping position of the flexible fixture and the vibration modes of the cockpit cover during the manufacturing process.

## Data Availability

The data used to support the findings of this study are included within the article.

## Conflicts of Interest

The authors declare that they have no conflicts of interest.

## Acknowledgments

The authors are grateful for the support by the National Science Foundation of China (grant. no. 91948203), project funded by China Postdoctoral Science Foundation (2019M651145), the State Key Laboratory of Robotics (2019-O21), and Natural Science Foundation of Liaoning Province (2019-ZD-0663).

## References

- [1] L. Jiang, Y. Li, L. Han, Y. Zou, G. Ding, and S. Qin, "A workpiece registration and localization adjustment method with contact inspection under multi-tolerance conditions," *Proceedings of the Institution of Mechanical Engineers, Part B: Journal of Engineering Manufacture*, vol. 233, no. 6, pp. 1653–1662, 2019.
- [2] J. Fei, F. Xu, B. Lin et al., "State of the art in milling process of the flexible workpiece," *International Journal of Advanced Manufacturing Technology*, vol. 109, p. 1725, 2020.

- [3] Z. Ahmad, T. Sultan, M. Asad, M. Zoppi, and R. Molino, "Fixture layout optimization for multi point respot welding of sheet metals," *Journal of Mechanical Science and Technology*, vol. 32, no. 4, pp. 1749–1760, 2018.
- [4] L. Zhan and K. Zhou, "Adaptive fuzzy sliding mode control for a robotic aircraft flexible tooling system," *International Journal of Advanced Manufacturing Technology*, vol. 69, no. 5–8, pp. 1469–1481, 2013.
- [5] H. Zhou, D. Wei, Y. Chen, and F. Wu, "Promoting mutual adaptation in haptic negotiation using adaptive virtual fixture," *Industrial Robot*, 2021.
- [6] V. Sabri, S. A. Tahan, X. T. Pham, D. Moreau, and S. Galibois, "Fixtureless profile inspection of non-rigid parts using the numerical inspection fixture with improved definition of displacement boundary conditions," *The International Journal of Advanced Manufacturing Technology*, vol. 82, no. 5–8, pp. 1343–1352, 2016.
- [7] M. D. Do, M. Kim, D. H. Nguyen, and H.-J. Choi, "Augmented-reality-assisted workpiece localization in rod-type flexible fixtures," *Journal of Mechanical Science and Technology*, vol. 34, no. 7, pp. 3007–3013, 2020.
- [8] X. Hao, Y. Li, T. Deng, C. Liu, and B. Xiang, "Tool path transplantation method for adaptive machining of large-sized and thin-walled free form surface parts based on error distribution," *Robotics and Computer-Integrated Manufacturing*, vol. 56, pp. 222–232, 2019.
- [9] J. Xu, W. Hou, Y. Sun, and Y.-S. Lee, "PLSP based layered contour generation from point cloud for additive manufacturing," *Robotics and Computer-Integrated Manufacturing*, vol. 49, pp. 1–12, 2018.
- [10] J. T. Xu, L. K. Xu, Y. W. Sun, Y. S. Lee, and J. B. Zhao, "A method of generating spiral tool path for direct three-axis computer numerical control machining of measured cloud of point," *Journal of Computing and Information Science in Engineering*, vol. 19, no. 4, pp. 1–12, 2019.
- [11] T. Gmeiner and K. Shea, "An ontology for the autonomous reconfiguration of a flexible fixture device," *Journal of Computing and Information Science in Engineering*, vol. 13, no. 2, pp. 1–12, 2013.
- [12] H. Wang, J. Peng, B. Zhao et al., "Modeling and performance analysis of machining fixture for near-net-shaped jet engine blade," *Assembly Automation*, vol. 39, no. 4, pp. 624–635, 2019.
- [13] C. Chen, Y. Sun, and J. Ni, "Optimization of flexible fixture layout using N-M principle," *The International Journal of Advanced Manufacturing Technology*, vol. 96, no. 9–12, pp. 4303–4311, 2018.
- [14] Z. Jiang and X. Tang, "Optimization of fixture flexibility for irregular geometries of workpiece based on metamorphic mechanisms," *International Journal of Advanced Manufacturing Technology*, vol. 103, pp. 325–342, 2019.
- [15] J. Ma, D. Zhang, B. Wu, M. Luo, and Y. Liu, "Stability improvement and vibration suppression of the thin-walled workpiece in milling process via magnetorheological fluid flexible fixture," *The International Journal of Advanced Manufacturing Technology*, vol. 88, no. 5–8, pp. 1231–1242, 2017.
- [16] P. Bergström and O. Edlund, "Robust registration of point sets using iteratively reweighted least squares," *Computational Optimization and Applications*, vol. 58, no. 3, pp. 543–561, 2014.
- [17] X. Wang, P. Ma, X. Peng, and S. Ning, "Study on vibration suppression performance of a flexible fixture for a thin-walled casing," *The International Journal of Advanced Manufacturing Technology*, vol. 106, no. 9–10, pp. 4281–4291, 2020.
- [18] A. Lang, Z. Song, G. He, and Y. Sang, "Profile error evaluation of free-form surface using sequential quadratic programming algorithm," *Precision Engineering*, vol. 47, pp. 344–352, 2017.
- [19] P. Löschner, K. Jarosz, and P. Nieslony, "Investigation of the effect of workpiece resolution on milling simulation accuracy in production module 3D CAE software," *Technical Gazette*, vol. 25, no. 5, pp. 1384–1388, 2018.